Article

Cell Reports

ASIC3 Mediates Itch Sensation in Response to Coincident Stimulation by Acid and Nonproton Ligand

Graphical Abstract

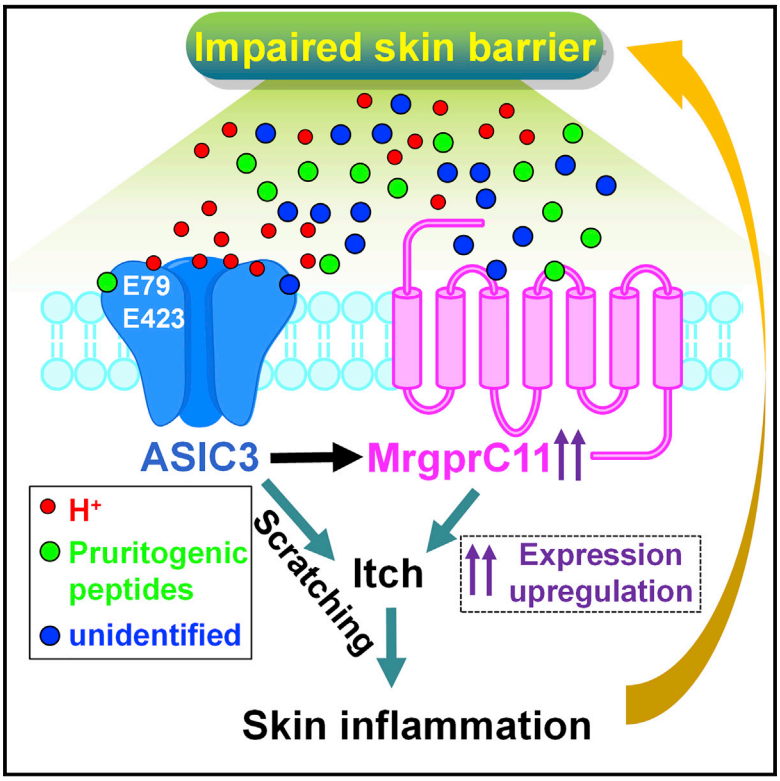

Authors

Zhong Peng, Wei-Guang Li, Chen Huang, ..., Michael Xi Zhu, Xiaoyang Cheng, Tian-Le Xu

Correspondence

xycheng@shsmu.edu.cn (X.C.), xu-happiness@shsmu.edu.cn (T.X.)

In Brief

Peng et al. show that pathological acidosis facilitates pruritogenic itch transduction via ASIC3. The nonproton ligand-sensing domain of ASIC3 is directly involved in sensing pruritogens and thereby attenuating channel desensitization. The study reveals a mechanism by which ASIC3 mediates both pain and itch under pathological conditions associated with inflammation and tissue injury.

Highlights

- Acidosis enhances certain pruritogenic itch via ASIC3
- Pruritogen SL-NH_2 acts at ASIC3 to slow channel desensitization
- Compounds that cause sustained ASIC3 currents induce an itch response
- ASIC3 is critical for scratching behavior and pathological changes in chronic itch

Peng et al., 2015, Cell Reports *13*, 387–398
October 13, 2015
http://dx.doi.org/10.1016/j.celrep.2015.09.002

Cell Reports
Article

ASIC3 Mediates Itch Sensation in Response to Coincident Stimulation by Acid and Nonproton Ligand

Zhong Peng,[1,3] Wei-Guang Li,[1,3] Chen Huang,[1] Yi-Ming Jiang,[1] Xiang Wang,[1] Michael Xi Zhu,[2] Xiaoyang Cheng,[1,*] and Tian-Le Xu[1,*]

[1]Discipline of Neuroscience and Department of Anatomy, Histology and Embryology, Collaborative Innovation Center for Brain Science, Shanghai Key Laboratory for Tumor Microenvironment and Inflammation, Shanghai Jiao Tong University School of Medicine, Shanghai 200025, China

[2]Department of Integrative Biology and Pharmacology, University of Texas Health Science Center, Houston, TX 77030, USA

[3]Co-first author

*Correspondence: xycheng@shsmu.edu.cn (X.C.), xu-happiness@shsmu.edu.cn (T.-L.X.)

http://dx.doi.org/10.1016/j.celrep.2015.09.002

SUMMARY

The regulation and mechanisms underlying itch sensation are complex. Here, we report a role for acid-sensing ion channel 3 (ASIC3) in mediating itch evoked by certain pruritogens during tissue acidosis. Co-administration of acid with Ser-Leu-Ile-Gly-Arg-Leu-NH_2 (SL-NH_2) increased scratching behavior in wild-type, but not ASIC3-null, mice, implicating the channel in coincident detection of acidosis and pruritogens. Mechanistically, SL-NH_2 slowed desensitization of proton-evoked currents by targeting the previously identified nonproton ligand-sensing domain located in the extracellular region of ASIC3 channels in primary sensory neurons. Ablation of the ASIC3 gene reduced dry-skin-induced scratching behavior and pathological changes under conditions with concomitant inflammation. Taken together, our data suggest that ASIC3 mediates itch sensation via coincident detection of acidosis and nonproton ligands that act at the nonproton ligand-sensing domain of the channel.

INTRODUCTION

Itch, also termed pruritus, is defined as an unpleasant sensation that evokes a desire to scratch (Ikoma et al., 2006). Studies to elucidate the mechanisms of itch have led to a dichotomy of histaminergic and histamine-independent itch. Being the best understood pruritogen, histamine is released from immune cells and keratinocytes and acts on a subset of sensory neurons that express both histamine receptors and TRPV1 channels to evoke itch (Imamachi et al., 2009; Shim et al., 2007). However, many forms of itch are insensitive to antihistamine treatment. The mechanisms of non-histaminergic itch have been intensively investigated over the past several years (Bautista et al., 2014; Han and Dong, 2014; LaMotte et al., 2014). Recently, a novel class of histamine-independent itch receptors, belonging to the Mas-related G-protein-coupled receptor (Mrgpr) family, has been identified. Expressed specifically in sensory neurons, Mrgprs can be activated by a large body of endogenous and exogenous pruritogens. While MrgprA3 is a receptor crucial for itch induced by the antimalarial drug chloroquine (Liu et al., 2009), MrgprD mediates β-alanine-evoked itch, mild prickling, tingling, and burning sensations (Liu et al., 2012). MrgprC11 is the receptor (Liu et al., 2009) for the endogenous bovine adrenal medulla 8-22 peptide (BAM8-22), a proteolytically cleaved product (Lembo et al., 2002) of proenkephalin A. MrgprC11 is also responsible for the itch sensation (Liu et al., 2011) induced by the peptide Ser-Leu-Ile-Gly-Arg-Leu-NH_2 (SL-NH_2). Notably, Ser-Leu-Ile-Gly-Arg-Leu (SLIGRL) is a tethered ligand sequence of proteinase-activated receptor 2 (PAR2), which can be unmasked by serine proteases to self-activate PAR2 (Ramachandran and Hollenberg, 2008). Similarly, SL-NH_2 also activates PAR2 in the absence of proteases, a process that does not induce itch (Liu et al., 2011). Thus, Mrgprs form an itch receptor family in primary sensory neurons, with different members detecting different pruritogens. However, the regulation and underlying mechanisms of itch sensation under various physiological and pathological conditions (Qu et al., 2014) remain largely unexplored. Acidosis is a common condition associated with tissue injury and/or inflammation. Although it is well known to trigger pain sensation (Frey Law et al., 2008; Reeh and Steen, 1996; Steen and Reeh, 1993), its role in itch sensation remains mysterious.

Tissue acidosis is sufficient to activate one emerging class of membrane receptors known as the acid-sensing ion channels (ASICs) (Krishtal, 2003; Waldmann et al., 1997b), which belong to the epithelial sodium channel/degenerin (ENaC/DEG) protein family (Kellenberger and Schild, 2015). Molecular cloning has revealed four genes that give rise to at least six ASIC subunits (ASIC1a, 1b, 2a, 2b, 3, and 4), which form either homotrimeric or heterotrimeric channel complexes. The differences in expression and distribution of ASIC subunits, together with the variations in subunit composition and channel gating, contribute to the multi-modality in channel functions. ASIC1a is distributed throughout the central and peripheral nervous systems, participating in synaptic transmission and plasticity (Chiang et al.,

2015; Du et al., 2014; Kreple et al., 2014; Wemmie et al., 2002). Dysfunction of ASIC1a is associated with the development of diverse neurological diseases, including ischemic neuronal cell death (Gao et al., 2005; Xiong et al., 2004), epileptic seizure (Ziemann et al., 2008), and neurodegenerative diseases (Friese et al., 2007; Vergo et al., 2011). On the other hand, ASIC3 is widely expressed in peripheral sensory neurons and non-neuronal tissues, where it is implicated in multimodal sensory perception (Li and Xu, 2011), including nociception (Chen et al., 2002; Deval et al., 2008; Sluka et al., 2003), mechanosensation (Fromy et al., 2012; Price et al., 2001), and chemosensation (Birdsong et al., 2010; Sutherland et al., 2001).

In addition to activation by extracellular protons, ASIC3 channels can also be activated by nonproton ligands, such as the synthetic compound, 2-guainidinie-4-methylquinazoline (GMQ), which causes persistent activation of ASIC3 at neutral pH (Yu et al., 2010) through binding to an extracellular domain (Yu et al., 2011). The nonproton ligand-sensing domain of ASIC3 is also involved in sensing serotonin (5-HT), a classic inflammatory mediator that facilitates acid-induced peripheral pain sensitivity (Wang et al., 2013). Similarly, the Texas coral snake toxin, MitTx-α/β, directly activates peripheral ASIC1a channels to elicit robust pain-related behaviors in mice (Bohlen et al., 2011) through extensive interactions with the extracellular region of the channel (Baconguis et al., 2014). Taken together, ASICs act as multimodal receptors that sense chemical stimuli, in addition to protons, from the extracellular environment. Considering the chemosensory nature of itch sensation, we examined the potential contribution of ASICs in itch transduction. Here, we report that ASIC3 channels play a critical role in promoting itch behavior through coincident detection of acidosis and certain pruritogens that act at the nonproton ligand-sensing domain of the channel.

RESULTS

Acidosis Potentiates SL-NH_2-Evoked, but Not BAM8-22-Evoked, Itch through ASIC3

To explore the potential roles of ASIC3 channels in itch sensation, we first examined the possibility that extracellular protons act as a pruritogen. Subcutaneous injection of an acidic solution (pH ~3.5–4.0) into the nape of the neck evoked minimal scratching behaviors compared to saline-injected mice (Figures 1A, 1D, and 1E), suggesting that proton alone is not a pruritogen. A two-way ANOVA conducted on the scratching bouts within each 5-min bin over the whole 30-min period indicated no significant difference between wild-type (WT) and ASIC3 knockout (KO) mice (WT versus ASIC KO, $F_{(1,138)} = 0.007$, $p = 0.933$; Figure 1A). Next, we investigated whether ASIC3 participates in itch evoked by known pruritogens. The MrgprC11 agonists SL-NH_2 (Figures 1A, 1D, and 1E) and BAM8-22 (Figures 1F–1H) induced scratching behavior in both WT and ASIC3 KO mice, with no significant difference between groups in the total number of scratching bouts over a period of 30 min after pruritogen injection. Further analysis on scratching bouts within each 5-min bin during the 30-min test (SL-NH_2: WT versus ASIC3 KO, $F_{(1,138)} = 0.442$, $p = 0.507$, Figure 1A; BAM8-22: WT versus ASIC3 KO, $F_{(1,144)} = 1.090$, $p = 0.298$, Figure 1F) suggested no significant roles of ASIC3 in the transduction of MrgprC11-dependent itch.

However, when co-injected with SL-NH_2, acetic acid (10 mM; 0.6%, v/v) enhanced itch behavior compared with the pruritogen alone in WT, but not ASIC3 KO, mice (Figures 1B, 1D, and 1E), suggesting that acid potentiates SL-NH_2-evoked itch and that ASIC3 is essential for such an effect (SL-NH_2 + acid: WT versus ASIC3 KO, $F_{(1,144)} = 20.085$, $p < 0.001$; Figure 1B). Application of amiloride (AMI), a nonselective inhibitor of ASICs, eliminated the ASIC3-dependent potentiation of SL-NH_2-evoked itch response by acid (SL-NH_2 + acid + AMI: WT versus ASIC3 KO, $F_{(1,126)} = 0.022$, $p = 0.882$; Figure 1C). By contrast, no difference was observed between WT and ASIC3-deficient littermates (Figures 1F–1H) either over the entire 30 min following co-injection of acid and BAM8-22 or within each 5-min bin during the 30-min test period (BAM8-22 + acid: WT versus ASIC3 KO, $F_{(1,108)} = 1.476$, $p = 0.227$), arguing for an MrgprC11-independent mechanism. Together, these results demonstrate that ASIC3 channels rather than MrgprC11 signaling play a critical role in synergizing SL-NH_2-evoked itch behavior in the presence of acidosis.

Importance of pH Dynamics for Acid Potentiation of SL-NH_2-Evoked Itch

Notably, the acid potentiation of SL-NH_2-evoked itch was only prominent within the first 5 min of co-injection and then quickly subsided afterward (Figure 1B) so that the cumulative scratch numbers over the 30-min test period were no longer significantly different between WT mice treated with SL-NH_2 alone and SL-NH_2 plus acid (Figure 1E). We reasoned that the quick decline of the acid potentiation effect might be because protons are easily buffered in the tissue in vivo. To test this possibility, we increased the pH-buffering capacity of the acidic solution using a high concentration (150 mM) of 2-(N-morpholino)ethanesulfonic acid (MES), an amphoteric compound that contains a sulfonic acid group and a tertiary amine group and is widely used to maintain the acidic pH in solutions. As shown in Figure S1, significant increases in scratch numbers were observed not only during the first 5 min (Figure S1C) but also within the entire 30-min test period (Figure S1D) following neck injection of SL-NH_2 in MES-buffered acidic solution as compared with the injection of the peptide at neutral pH. These results indicate that the potentiation of SL-NH_2-caused itch by acidosis depends on the extent and duration of sustained tissue acidosis, a condition that usually happens in inflammatory processes (Frey Law et al., 2008; Reeh and Steen, 1996; Steen and Reeh, 1993). By participating in the acidic regulation of pruritogenic itch, ASIC3 channels may be well positioned to influence pathophysiological itch during tissue injury and/or inflammation, in addition to pain.

Characterization of Acid Potentiation of SL-NH_2-Evoked Itch over Pain

To distinguish acid-potentiated itch from pain behaviors, we employed the cheek assay to analyze contributions of combined acidosis and pruritogens to itch and pain sensations. It has been shown that in the cheek model of acute itch, injection of algogens triggers wiping with the forelimbs, whereas injection of pruritogens leads to scratching with the hindlimbs (Shimada

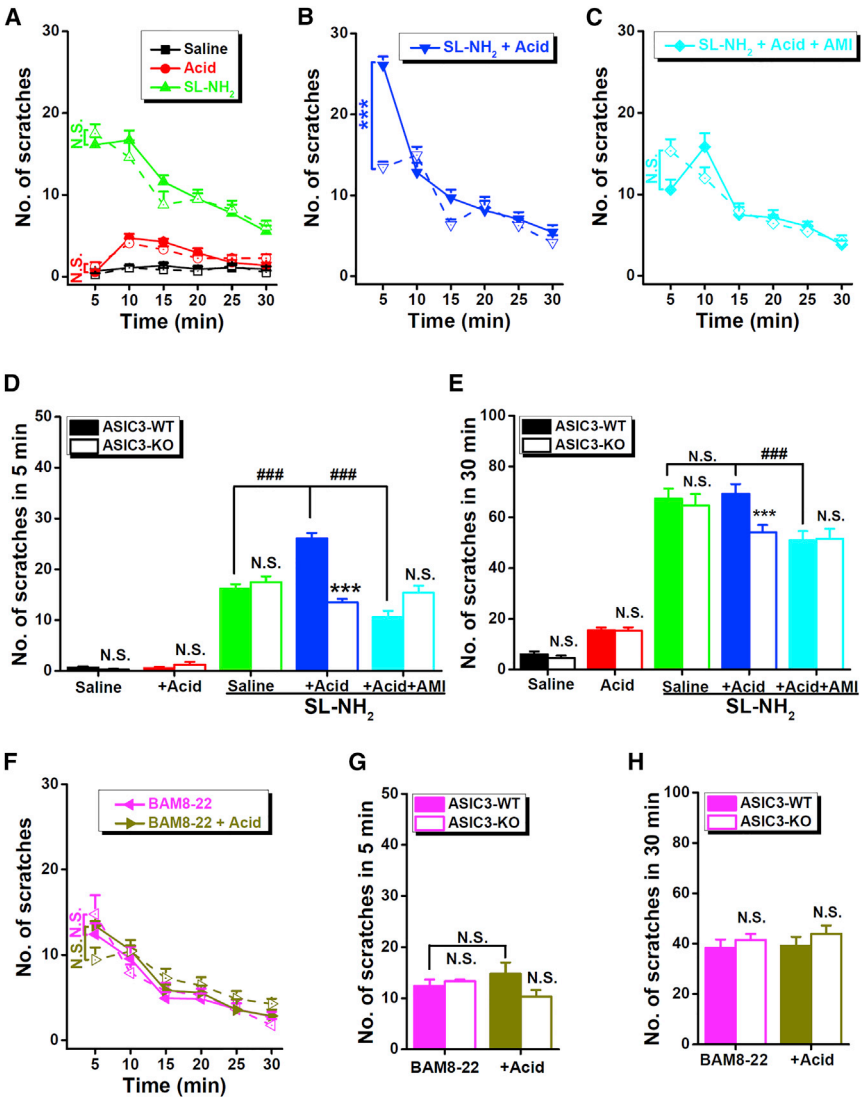

Figure 1. ASIC3 Is Involved in Acid Potentiation of SL-NH_2-Evoked Itch

Itch-related behavior in WT (filled) and ASIC3 KO (blank) mice as determined by scratching bouts in 5-min bins during a 30-min period following injection of saline or pruritogens (50 μl) at the rostral back/neck. Data represent mean ± SEM; n = 9–13.

(A) Acid, acetic acid (0.6%, v/v, pH ~3.5–4.0) in saline; SL-NH_2, 7 mM in saline.

(B) SL-NH_2 + acid, SL-NH_2 (7 mM) plus acetic acid (0.6%, v/v) in saline.

(C) SL-NH_2 + acid + AMI, SL-NH_2 (7 mM), acetic acid (0.6%, v/v), plus amiloride (AMI, 200 μM) in saline.

(D) Regraphed data from (A–C) for the initial 5 min following injection for comparison.

(E) Pooled data from (A)–(C) for the entire 30-min period following injection.

(F) BAM8-22, 3 mM in saline; BAM8-22 + acid, BAM8-22 (3 mM) plus acetic acid (0.6%, v/v) in saline.

(G) Regraphed data from (F) for the initial 5 min following injection for comparison.

(H) Pooled data from (F) for the entire 30 min following injection.

N.S., not significant, WT versus ASIC3 KO, or compared as indicated; ***$p < 0.001$, WT versus ASIC3 KO; ###$p < 0.001$, compared as indicated, by unpaired Student's t test (D, E, G, and H) or two-way repeated-measures ANOVA followed by least significant difference (LSD) post hoc comparison (A–C and F).

See also Figures S1.

and LaMotte, 2008). Consistent with this notion and SL-NH_2 being a pruritogen (Akiyama et al., 2010), injection of SL-NH_2 to the cheek strongly evoked similar scratching responses in both WT and ASIC3 KO mice (Figure 2A), but to a much lesser extent than wiping responses (Figure 2B). By contrast, cheek injection of acid alone produced similar scratching responses between WT and ASIC3 KO mice (Figure 2A) but more pronounced wiping in WT mice than in ASIC3 KO mice (Figure 2B). This supports the role of ASIC3 in acid-induced pain; however, ASIC3 does not mediate itch sensation in the absence of pruritogens.

However, co-injection of acid and SL-NH_2 to the cheek significantly increased scratching behaviors (Figure 2A) in WT, but not ASIC3 KO, mice as compared with SL-NH_2 alone. The effect on scratching behavior was again abolished by co-injection of AMI (Figure 2A). These results are consistent with that obtained from the neck model of acute itch (Figures 1B and 1D), strengthening the notion that acidosis potentiates pruritogenic itch in an ASIC3-dependent manner. In addition, the co-injection of SL-NH_2 and acid also increased wiping behaviors as compared with the pruritogen or acid alone in WT, but not ASIC3 KO, mice (Figure 2B). The effect on wiping behavior in WT mice was also abolished by pharmacological inhibition of ASICs using AMI (Figure 2B). Collectively, these results suggest that ASIC3 channels mediate a complex pain and itch sensation in response to a coincident stimulation by acid and certain pruritogens.

ASIC1a Is Not Required for Acid Potentiation of SL-NH_2-Evoked Itch

Interestingly, ASIC1a KO mice exhibited similar scratching responses to acid or SL-NH_2 alone (Figures 3A, 3C, and 3D) but had enhanced itching behavior with the co-injection of acid and SL-NH_2 when compared with WT littermates (Figures 3B–3D), indicating that ASIC1a is not responsible for the acid potentiation of SL-NH_2-evoked itch sensation. To examine the possibility that ASIC3 upregulation might be responsible for the enhanced acid potentiation in ASIC1a KO mice, we analyzed mRNA levels of different ASIC subunits in dorsal root ganglion (DRG) from WT and ASIC1a KO mice. As shown in Figure S2, the mRNA levels of all ASIC subunits except ASIC1a remained unchanged in the ASIC1a-null mice, indicating that the increased

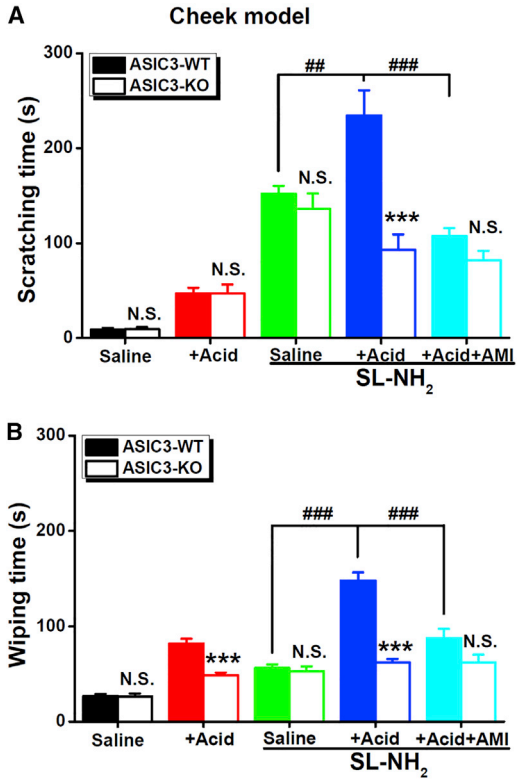

Figure 2. Characterization of Acid Potentiation of SL-NH_2-Evoked Itch over Pain

Itch- and pain-related behaviors in WT (filled) and ASIC3 KO (blank) mice as determined by the time spent on scratching using the hindlimbs (A) and wiping with the forelimbs (B), respectively, during the entire 30 min following injection of saline or pruritogens (10 μl) to the cheek. Data represent means ± SEM; n = 9–12. Acid, acetic acid (1.5%, v/v) in saline; SL-NH_2, 20 mM in saline; SL-NH_2 + acid, SL-NH_2 (20 mM) plus acetic acid (1.5%, v/v) in saline; SL-NH_2 + acid + AMI, SL-NH_2 (20 mM), acetic acid (1.5%, v/v) plus AMI (500 μM) in saline. N.S., not significant, WT versus ASIC3 KO; ***$p < 0.001$, WT versus ASIC3 KO; ##$p < 0.01$, ###$p < 0.001$, compared as indicated, by unpaired Student's t test.

scratching response to acid plus SL-NH_2 in ASIC1a KO mice was unlikely due to a compensatory change of ASIC3 in the sensory neurons. Nevertheless, these data strengthen the selective requirement of ASIC3, but not ASIC1a, for acid potentiation of SL-NH_2-evoked itch.

SL-NH_2, but Not BAM8-22, Reduces the Desensitization Rate of Acid-Induced ASIC3 Current

To explore the mechanism(s) underlying the synergistic effects between acid and SL-NH_2 on itch sensation, we examined the acute effects of SL-NH_2 or BAM8-22 on proton-evoked currents in Chinese hamster ovary (CHO) cells expressing ASIC3 using whole-cell patch-clamp recording. As previously reported (Waldmann et al., 1997a; Yu et al., 2010), lowering the extracellular pH from 7.4 to 5.0 elicited a rapidly activating current followed by fast desensitization (Figure 4A). When applied alone, neither SL-NH_2 nor BAM8-22 generated any current in CHO cells expressing ASIC3 (Figure 4A). However, SL-NH_2 (100 μM), but not BAM8-22 (30 μM), dramatically impeded the desensitization of pH-5.0-induced currents (Figures 4A and 4B) without affecting the peak current amplitude (100.5% ± 1.0% and 101.0% ± 0.7% of pH-5.0-evoked current in the presence of SL-NH_2 and BAM8-22, respectively, n = 8–9, $p > 0.05$, paired Student's t test). The selective modulation of ASIC3 desensitization by SL-NH_2 may explain the acidosis-enhanced itch response by SL-NH_2, but not BAM8-22 (Figures 1F–1H).

Characterization of SL-NH_2 Modulation on Acid-Induced ASIC3 Current

To further characterize the effects of SL-NH_2 on acid-induced ASIC3 activation and desensitization, we recorded ASIC3 currents at different concentrations of SL-NH_2. In CHO cells expressing ASIC3 channels, SL-NH_2 dose-dependently reduced the rate of desensitization of pH-5.0-induced currents (Figures S3A and S3B) without affecting the peak current amplitude (Figure S3C). We also tested the pH dependence of SL-NH_2-mediated modulation of proton-induced ASIC3 currents, and we noted that the effect of SL-NH_2 on ASIC3 desensitization became more pronounced as the pH decreased (Figures S3D and S3E), with negligible influence on the peak amplitude at all pH values tested (Figure S3F). Therefore, the modulation of ASIC3 desensitization is dependent on both proton and SL-NH_2 concentrations.

SL-NH_2 activates both MrgprC11 and PAR2 receptors. However, the effect of SL-NH_2 on ASIC3 currents recorded from CHO cells is unlikely related to PAR2 (Ramachandran and Hollenberg, 2008), because there is no endogenous PAR2 in these cells (Nystedt et al., 1995). Also, MrgprC11 is sensory-neuron specific (Liu et al., 2009; Liu et al., 2011) and unlikely present in CHO cells. To test whether SL-NH_2 acts directly at ASIC3 channels, we first examined whether the effect of SL-NH_2 on the acid-induced ASIC3 current required any intracellular molecule using excised outside-out patches, in which diffusible intracellular molecules would mostly be lost. Similar to what was observed in whole-cell recordings, SL-NH_2 (100 μM) significantly reduced the rate of desensitization of acid-induced current in outside-out patches excised from CHO cells that expressed ASIC3 (Figures S4A and S4B) without affecting the peak current amplitude (Figure S4C), consistent with a direct interaction between SL-NH_2 and ASIC3 channels.

Critical Role of the Nonproton Ligand-Sensing Domain for SL-NH_2 Modulation of ASIC3 Current

The acute and possibly direct modulation of ASIC3 currents by SL-NH_2 prompted us to explore the structural basis of this interaction. As previously reported, in addition to its effect on the sustained activation of ASIC3 induced by acid (Wang et al., 2013) and nonproton ligands (Yu et al., 2010), the nonproton ligand-sensing domain located in the extracellular region of ASIC3 channels (Yu et al., 2011) plays a critical role in the desensitization of proton-evoked currents (Cushman et al., 2007). Given that the modulation of ASIC3 currents by SL-NH_2 and 5-HT was similar (Wang et al., 2013), we reasoned that just like 5-HT, the nonproton ligand-sensing domain could also be involved in the modulation of currents by SL-NH_2. Supporting this idea, we found that similar to the sustained activation (Yu et al., 2010) and modulation (Wang et al., 2013) by other nonproton ligands,

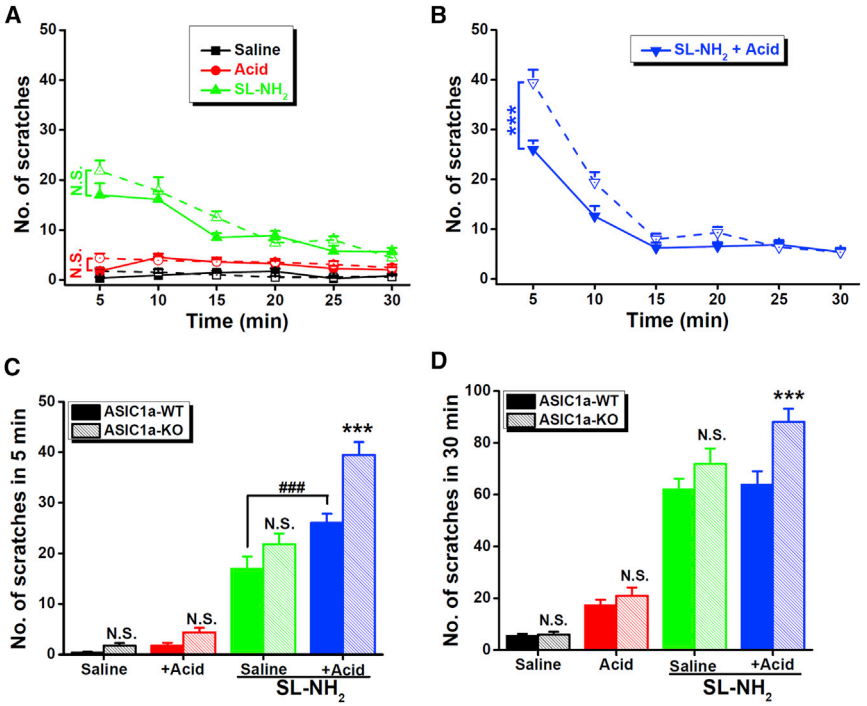

Figure 3. Effects of Acidosis on SL-NH_2-Evoked Itch in WT and ASIC1a KO Mice

Itch-related behaviors as determined by the scratching bouts in 5-min bins during the 30 min following injection of saline or compounds (50 μl) to the rostral back/neck of WT (filled) and ASIC1a KO (patterned) mice. Data represent the mean ± SEM n = 8–12.

(A) Acid, acetic acid (0.6%, v/v, pH ~3.5–4.0) in saline; SL-NH_2, 7 mM in saline.

(B) SL-NH_2 + Acid, SL-NH_2 (7 mM) plus acetic acid (0.6%, v/v) in saline.

(C) Regraphed data from (A and B) for the initial 5 min following injection for comparison.

(D) Pooled data from (A and B) for the entire 30 min following injection.

N.S., not significant; ***$p < 0.001$, WT (filled) versus ASIC1a KO (patterned); $^{###}p < 0.001$, compared as indicated, by unpaired Student's t test (C and D) or two-way repeated-measures ANOVA (A and B). See also Figures S2.

glutamate 79 (E79) and glutamate 423 (E423) were essential for the modulation of ASIC3 currents by SL-NH_2 (Figures 4C and S4D). When E79 was substituted with cysteine (C), glutamine (Q), or serine (S), the mutated channel became largely insensitive to SL-NH_2 (Figures 4C and S4D). Similar results were obtained when E423 was replaced with alanine (A), C, or Q (Figures 4C and S4D). Because of the strong steady-state desensitization (Cushman et al., 2007; Yu et al., 2010), we did not test the effects of SL-NH_2 on the E79A mutant. In addition, except for E79C, SL-NH_2 did not change the proton-evoked current amplitude of mutant channels (Figure S4E). These results demonstrate that the nonproton ligand-sensing domain is critical for SL-NH_2-mediated modulation of ASIC3 currents.

Next, we looked into the structure-activity relationship of SL-NH_2 on ASIC3 channels using a series of SL-NH_2 analogs (Figures 4D and S5A). When the positively charged arginine of SL-NH_2 was replaced by the acidic glutamate (E) or the neutral isoleucine (I) residue, the resulting peptide, SLIG*E*L-NH_2 or SLIG*I*L-NH_2, lost the ability to reduce the rate of ASIC3 desensitization (Figures 4D and S5B) during acid exposure. When the arginine was substituted with positively charged lysine (*K*) or histidine (*H*), the resulting peptide, SLIG*K*L-NH_2 or SLIG*H*L-NH_2, partially preserved the modulation on channel desensitization despite the substantially weaker effect when compared with SL-NH_2 (Figures 4D and S5B), indicating that both the positive charge and the stereochemistry of the arginine residue in SL-NH_2 are required for impeding ASIC3 desensitization. In contrast, peptides with substitutions of other residues in SL-NH_2 produced similar or even stronger effects on ASIC3 desensitization than SL-NH_2, suggesting less involvement of these residues in the interaction between SL-NH_2 and ASIC3 (Figures 4D and S5C). Of note, when the flexible glycine residue was replaced by alanine, presumably introducing an additional steric hindrance, the resulting peptide, SLI*A*RL-NH_2, displayed a more pronounced inhibition on the desensitization of ASIC3 currents than SL-NH_2 (Figures 4D and S5C), supporting that electrostatic and steric interactions are both required for the inhibition of ASIC3 channel desensitization by SL-NH_2. Importantly, none of the SL-NH_2 analogs had any effect on the peak amplitude of ASIC3 current (Figure S5D).

SL-NH_2 Prolongs Acid-Induced Currents in Sensory Neurons

To gain insight into the physiological function of the ASIC3-dependent synergism of SL-NH_2 and acidosis, we investigated the effect of SL-NH_2 on DRG neurons, where functional ASIC3 channels are abundant (Waldmann et al., 1997a). Because TRPV1 channels can also be activated by protons, AMG9810 (10 μM), a TRPV1 antagonist (Gavva et al., 2005), was added into the bath solution to prevent TRPV1 activation. Consistent with previous studies (Wang et al., 2013), whole-cell recordings revealed that pH 5.0 evoked rapidly desensitizing ASIC-like currents in 80.1% (109/136) small- and medium-sized (15–30 μm diameters) DRG neurons from WT mice. To minimize the variation in current density, only neurons producing robust ASIC-like currents (peak amplitude >1 nA) were used to further test the effect of SL-NH_2. Application of SL-NH_2 dose-dependently impeded the desensitization of acid-evoked currents in WT neurons (85.7% [six out of seven]) (Figures 4E and S6A). By contrast, no effect was detected for 100 μM SL-NH_2 in ASIC3 KO neurons (Figures 4E and S6A). As expected, SL-NH_2 did not affect the peak amplitude of any ASIC current examined (Figure S6B). These data support the notion that SL-NH_2 impedes the desensitization of acid-evoked currents in native DRG neurons by selectively acting at ASIC3 channels.

Because of the heterogeneity of ASIC isoforms in primary sensory neurons (Alvarez de la Rosa et al., 2002), we verified the

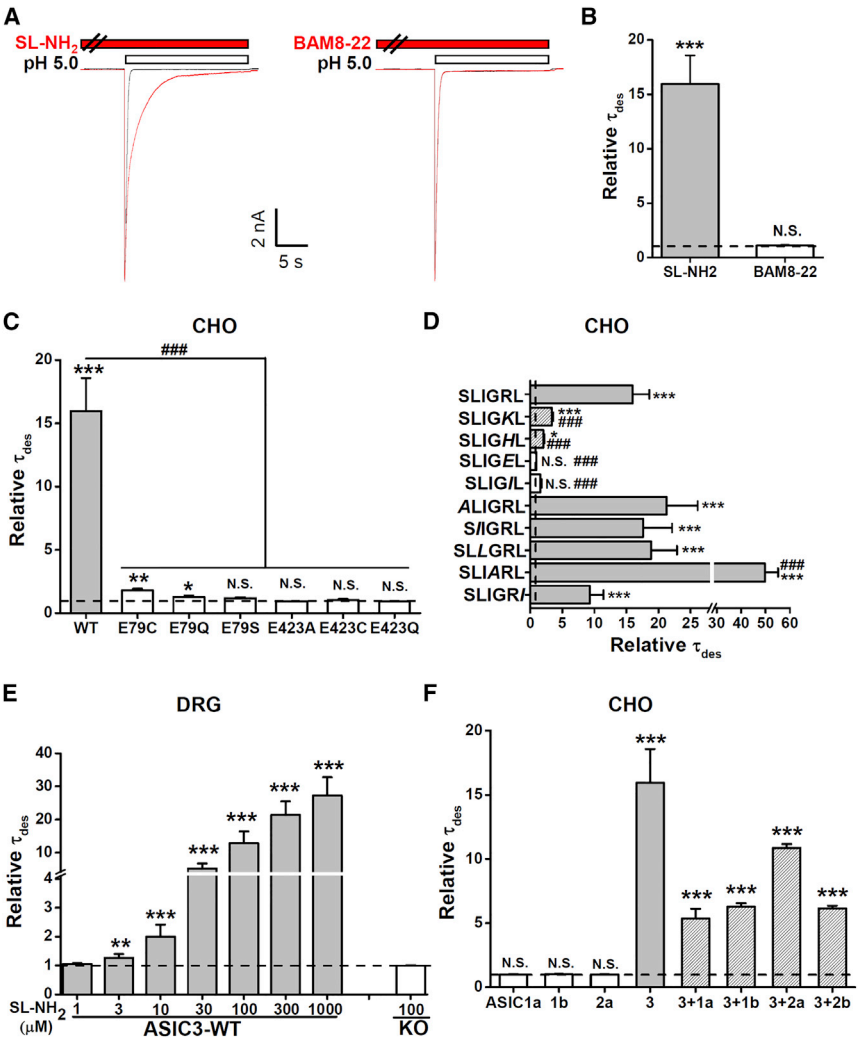

Figure 4. SL-NH_2 Slows the Rate of Desensitization of Acid-Induced ASIC3 Current

(A) Representative traces of currents induced by pH 5.0 in the absence (black) and presence (red) of the indicated pruritogens in CHO cells expressing ASIC3. SL-NH_2, 100 μM; BAM8-22, 30 μM.

(B) Relative time constants of desensitization (τ_{des}) of pH-5.0-induced ASIC3 current in the presence of SL-NH_2 and BAM8-22 normalized to that in the absence of the peptides for the same cell. Data represent means ± SEM; n = 7. N.S., not significant; ***p < 0.001, compared with τ_{des} induced by pH 5.0 alone (dashed line), by paired Student's t test.

(C) Effects of the nonproton ligand-sensing domain of ASIC3 on SL-NH_2 modulation of pH-5.0-induced ASIC3 currents. Data are means ± SEM of τ_{des} of proton-induced currents in the presence of SL-NH_2 (100 μM) normalized to that induced by pH 5.0 alone (dashed line) for CHO cells that expressed WT ASIC3 and its mutants affecting the key residues (E79 and E423) that define the nonproton ligand-sensing domain. Representative current traces are shown in Figure S4D. Data for WT ASIC3 are from (B), regraphed for comparison. n = 5–8. *p < 0.05, **p < 0.01, ***p < 0.001 compared with the relative τ_{des} induced by acid alone (dashed line), by paired Student's t test. ###p < 0.001, compared with WT, by unpaired Student's t test.

(D) Structure-activity relationship of SL-NH_2 derivatives modulating desensitization of acid-induced ASIC3 currents. Data are means ± SEM of τ_{des} of proton-induced currents in the presence of the indicated SL-NH_2 derivatives (100 μM) normalized to that induced by pH 5.0 alone (dashed line) for CHO cells that expressed WT ASIC3. Representative current traces are shown in Figures S5B and S5C. Data for SL-NH_2 (i.e., SLIGRL) are from (B), regraphed for comparison. n = 6–9. *p < 0.05, ***p < 0.001, compared with the relative τ_{des} induced by acid alone (dashed line), by paired Student's t test; ###p < 0.001, compared with SL-NH_2 (i.e., SLIGRL), by unpaired Student's t test.

(E) Effects of SL-NH_2 on acid-induced currents in sensory neurons from WT or ASIC3 KO mice. Data are means ± SEM of τ_{des} of proton-induced currents in the presence of indicated concentrations of SL-NH_2 normalized to that induced by pH 5.0 alone (dashed line) in WT and ASIC3 KO DRG neurons. Representative current traces are shown in Figure S6A. n = 5–6. **p < 0.01, ***p < 0.001, compared with the relative τ_{des} induced by acid alone (dashed line), by paired Student's t test.

(F) Isoform specificity of SL-NH_2 modulation on ASICs. Data are means ± SEM of τ_{des} of proton-induced currents in the presence of SL-NH_2 (100 μM) normalized to that induced by pH 5.0 alone (dashed line) in CHO cells that expressed ASIC subtypes as indicated. Representative current traces are shown in Figure S6C. Data for ASIC3 were from (B), regraphed for comparison. n = 6–9. ***p < 0.001, compared with the relative τ_{des} induced by acid alone (dashed line), by paired Student's t test.

See also Figures S3–S6.

selectivity of SL-NH_2 using CHO cells expressing specific ASIC isoforms. As shown in Figures 4F and S6C, SL-NH_2 (100 μM) did not affect desensitization of acid-induced currents in CHO cells expressing homomeric ASIC1a, ASIC1b, or ASIC2a channels, whereas it significantly reduced the rate of desensitization of all heteromeric channels containing ASIC3, despite being less pronounced than that of homomeric ASIC3 channels (Figures 4F and S6C). As expected, SL-NH_2 did not affect the peak amplitude of any ASIC current examined (Figure S6D). We conclude that SL-NH_2 selectively slows the desensitization of ASIC3-containing homomeric and heteromeric channels in both DRG neurons and CHO cells, leading to prolonged activation of the channel.

Prolonged Activation of ASIC3 Channels Is Sufficient to Cause Itch

To explore whether the prolonged activation of ASIC3 channels is sufficient to promote itch, we took advantage of the endogenous neuropeptide FF (NPFF), which potentiates ASIC3 activities by selectively enhancing the sustained component of acid-evoked current (Askwith et al., 2000) (Figures 5A and 5B). NPFF also exerts its effect on ASIC3 channels by acting at the nonproton ligand-sensing domain (data not shown). Interestingly, NPFF at neutral pH evoked similar itch responses in WT and ASIC3 KO mice (Figure 5C), indicative of an ASIC3-independent effect. However, co-injection of NPFF and acid

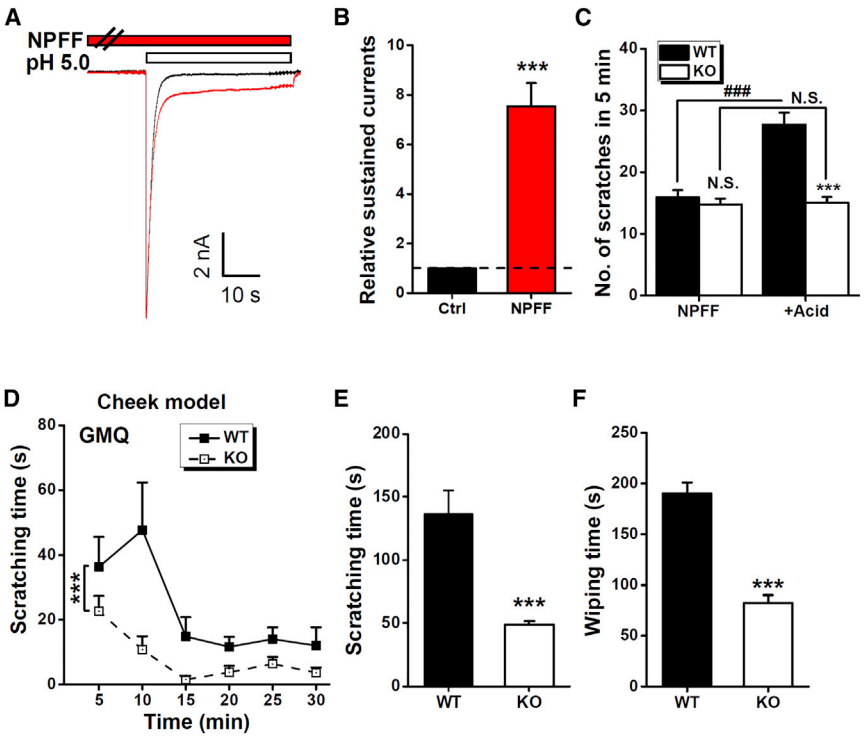

Figure 5. Compounds that Activate Sustained ASIC3 Currents Induce Itch Responses

(A–C) Effects of NPFF on the acid-evoked ASIC3 currents and scratching behaviors. (A) Representative current traces induced by pH 5.0 in the absence (black) and presence (red) of NPFF (100 μM) in CHO cells that expressed ASIC3. (B) Sustained ASIC3 current at 10 s of the exposure to pH 5.0 in the presence of NPFF normalized to that induced by pH 5.0 alone (dashed line). Data are means ± SEM; n = 5. ***$p < 0.001$, compared with value by pH 5.0 alone, by paired Student's t test. (C) Itch-related behavior in WT (filled) and ASIC3 KO (blank) mice as determined by the scratching bouts within 5 min following injection of 50 μl saline or NPFF (7 mM in saline) without or with acetic acid (0.6%, v/v) as indicated into the rostral back/neck. n = 10 for each group. N.S., not significant; ***$p < 0.001$, WT versus ASIC3 KO, by unpaired Student's t test; ###$p < 0.001$, compared as indicated, by unpaired Student's t test.

(D–F) Itch- and pain-related behavior in WT (filled) and ASIC3 KO (blank) mice as determined the time spent on scratching using the hindlimbs (D and E) and wiping using the forelimbs (F), respectively, in 5 min bins during the 30 min period (D) or through the entire 30 min (E and F) following injection of GMQ (10 μl, 10 mM) into a site of cheek. Data are means ± SEM n = 9–12. ***$p < 0.001$, WT versus ASIC3 KO, by two-way repeated-measures ANOVA (D) or unpaired Student's t test (E and F).

significantly enhanced itch response in WT, but not ASIC3 KO, mice (Figure 5C), suggesting that prolonged activation of ASIC3 channels by co-stimulation with acid and a ligand that acts at the nonproton ligand-sensing domain is sufficient to induce itch.

We previously showed that GMQ causes sustained activation of ASIC3 channels at neutral pH (Yu et al., 2010) via binding to the nonproton ligand-sensing domain (Yu et al., 2011). To determine if prolonged ASIC3 activation at neutral pH in the absence of a known pruritogen could elicit itch response, we examined the effect of GMQ in the cheek assay. As shown in Figures 5D–5F, injection of GMQ to cheek induced both scratching behaviors with the hindlimbs and wiping behaviors with the forelimbs, indicative of both itch and pain responses, respectively (Shimada and LaMotte, 2008). Importantly, both the itch (Figures 5D and 5E) and pain (Figure 5F) responses were significantly higher in WT mice than in ASIC3 KO mice. Thus, the ASIC3 activator GMQ acts both as an algogen and a pruritogen, and the effects were largely mediated by ASIC3. Altogether, the above data demonstrate that prolonged activation of ASIC3 channels by either the nonproton ligand (i.e., GMQ) alone or the coincident stimulation by acidosis and a compound that acts at the nonproton ligand-sensing domain is sufficient to cause itch sensation.

ASIC3 Is Required for Itch and Epidermal Thickening in a Dry Skin Pruritus Model

To investigate the pathophysiological roles of ASIC3 in itch transduction, we employed a mouse model of chronic itch adapted from a model of experimental dry skin (Miyamoto et al., 2002; Wilson et al., 2013). After treatment with acetone, ether, and water (AEW) in the rostral back/neck (Figures 6A and 6B), the mice developed marked scratching behavior (Figure 6C) on the fifth day of AEW treatment. However, ASIC3 KO littermates demonstrated significantly reduced scratching behaviors compared with WT mice when subjected to an identical AEW assay (Figure 6C), suggesting that ASIC3 is involved in dry-skin-evoked chronic itch response. We next investigated whether acute ASIC inhibition by AMI could attenuate AEW-evoked scratching. Subcutaneous injection of AMI on the fifth day of AEW treatment into the AEW-treated area significantly reduced itch behaviors (Figure S7A). Next, we tested whether preventing acidosis by increasing the tissue pH, a condition that blocks acid- and nonproton-ligand-dependent activation of ASIC3 channels (Yu et al., 2010), through administration of HCO_3^- to the AEW-treated skin site, could attenuate the itch response. As expected, treatment with HCO_3^- substantially decreased spontaneous scratching behaviors (Figure S7A). These data collectively indicate that activation of ASICs is necessary for itch transduction under chronic dry skin conditions.

Furthermore, AEW triggered a substantial increase in the thickness of nucleated epidermal layers compared with water-treated skin samples (Figures 6D and 6E). The epidermal hyperplasia was significantly less in ASIC3 KO mice than in WT controls (Figures 6D and 6E), suggesting that ASIC3 contributes to epidermal homeostasis in addition to the development of dry skin-induced chronic itch.

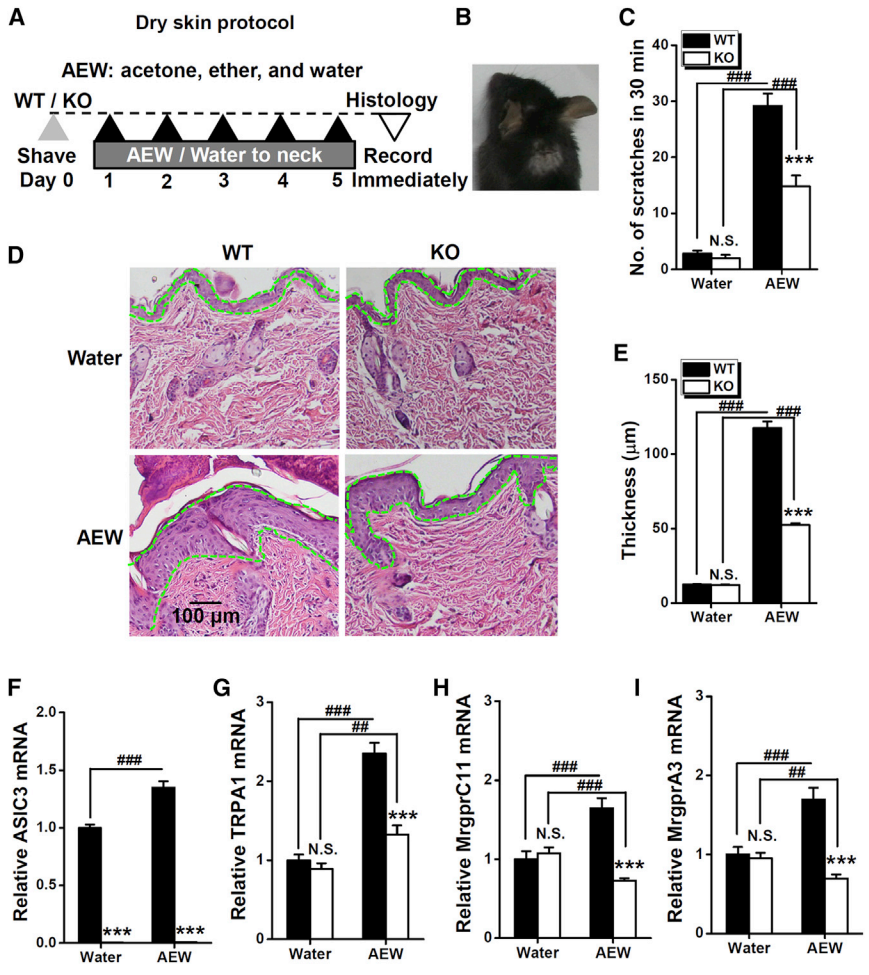

Figure 6. Contribution of ASIC3 to Dry-Skin-Induced Itch and Epidermal Hyperplasia in the Rostral Back/Neck Model

(A) Experimental scheme of the dry skin assay in mouse rostral back/neck. Scratching behaviors were recorded for 30 min on day 5 after the second AEW treatment (an 1:1 mixture of acetone and ether, followed by water). The treated skin area was removed for histological analysis following the recording on day 5.

(B) Representative image displaying the AEW-treated rostral back/neck area.

(C) Quantification of scratching bouts during the 30 min test. Data are means ± SEM; n = 10 for each group. N.S., not significant; ***p < 0.001, WT versus ASIC3 KO, by unpaired Student's t test; ###p < 0.001, compared as indicated, by unpaired Student's t test.

(D) Micrographic images of H&E-stained back/neck skin sections from WT and ASIC3 KO mice treated with water (upper) or AEW (lower).

(E) The thickness of nucleated epidermal layers was quantified for water- and AEW-treated skin samples. Data are means ± SEM; n = 10 for each group. N.S., not significant; ***p < 0.001, WT versus ASIC3 KO, by unpaired Student's t test; ###p < 0.001, compared as indicated, by unpaired Student's t test.

(F–I) Changes in mRNA expression of ASIC3 (F), TRPA1 (G), MrgprC11 (H), and MrgprA3 (I) in sensory neurons of WT and ASIC3 KO mice subjected to either water or AEW treatment, measured by quantitative real-time RT-PCR. The expression is reported as ΔΔCt, normalized to that of water-treated mice. n = 4 for each group. N.S., not significant; ***p < 0.001, WT versus ASIC3 KO, by unpaired Student's t test; ###p < 0.001, compared as indicated, by unpaired Student's t test.

See also Figure S7.

ASIC3 Is Required for Dry-Skin-Evoked Changes in Expression of Itch-Related Genes in Sensory Neurons

To gain insights into the molecular mechanisms by which ASIC3 contributes to chronic itch, we investigated whether dry skin alters gene expression in DRG neurons that innervate the mouse rostral back/neck. Using real-time RT-PCR, we detected an upregulation of ASIC3 mRNA in DRG neurons from AEW-treated WT mice as compared to water-treated mice (Figure 6F), supporting the notion that an active sensitization of ASIC3 occurs during the process of dry-skin-induced chronic itch. In addition, AEW treatment also significantly increased the expression of TRPA1 (Figure 6G), MrgprC11 (Figure 6H), and MrgprA3 (Figure 6I), all of which are critical components of histamine-independent itch transduction (Liu et al., 2009; Liu et al., 2011; Wilson et al., 2011) and known to contribute to dry-skin-induced chronic itch (Wilson et al., 2013). Notably, the upregulation of these genes was either largely suppressed (TRPA1) or completely prevented (MrgprC11 and MrgprA3) by the genetic deletion of ASIC3 (Figures 6G–6I), arguing for a critical role of ASIC3 in dry-skin-evoked changes in itch-related gene expression in the affected sensory neurons and dry-skin-induced chronic itch as well as the associated epidermal hyperplasia.

ASIC3-Mediated Skin Abnormality Is Scratching Dependent

To further define the role of ASIC3 in chronic itch, we recapitulated the phenotype of dry-skin-induced chronic itch and epidermal thickening in the cheek assay (Figures 7A and 7B). In response to daily cheek treatment with AEW, but not water, the mice developed marked spontaneous scratching (Figure 7C) as well as wiping behavior (Figure 7D) on the fifth day of the dry skin protocol. As expected, the ASIC3 KO littermates demonstrated significantly reduced scratching and wiping behaviors when subjected to an identical AEW assay (Figures 7C and 7D), validating that ASIC3 indeed significantly contributes to dry-skin-evoked abnormal sensory behaviors. Like in the rostral back/neck assay, AEW triggered a substantial increase in the thickness of nucleated epidermal layers of cheek skin compared with water-treated skin samples (Figures 7E and 7F). Importantly, ASIC3 KO mice showed significantly less epidermal hyperplasia than WT controls (Figures 7E and 7F), strengthening the role of ASIC3 in epidermal homeostatic regulation during chronic itch.

To further illuminate the mechanistic details of ASIC3-dependent epidermal hyperplasia that occurred upon dry skin

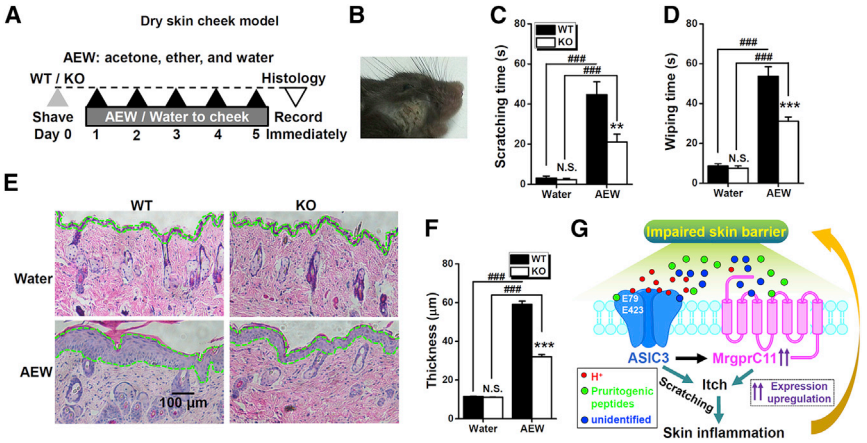

Figure 7. Contribution of ASIC3 to Dry-Skin-Induced Itch and Epidermal Hyperplasia in the Cheek Model

(A) Experimental scheme of the dry skin assay in mouse cheek. Scratching behaviors were recorded for 30 min on day 5 after the second AEW treatment. The treated skin area was removed for histological analysis following the recording on day 5.

(B) Representative image displaying the AEW-treated cheek area.

(C and D) Quantification of time durations spent on scratching with the hindlimbs (C) or wiping with the forelimbs (D) during the 30-min test. Data are means ± SEM; n = 8–10 for each group. N.S., not significant; $^{**}p < 0.01$, $^{***}p < 0.001$, WT versus ASIC3 KO, by unpaired Student's t test; $^{###}p < 0.001$, compared as indicated, by unpaired Student's t test.

(E) Micrographic image of H&E-stained cheek skin sections from WT and ASIC3 KO mice treated with water (upper) or AEW (lower).

(F) The thickness of nucleated epidermal layers was quantified from water- and AEW-treated cheek skin. Data are means ± SEM; n = 8–10 for each group. N.S., not significant, $^{***}p < 0.001$, WT versus ASIC3 KO, by unpaired Student's t test. $^{###}p < 0.001$, compared as indicated, by unpaired Student's t test.

(G) A hypothetical scheme for combined stimulation by acid and pruritogens that act at nonproton ligand-sensing domain of ASIC3 channels under dry skin conditions with impaired skin barrier. Pruritogenic peptides, such as RFamide, and other unidentified endogenous agents are released to activate not only the classical itch receptors (e.g., MrgprC11) but also ASIC3 when tissue acidosis emanates from inflammation because of scratching of the affected skin. Please see the text for more details.

See also Figure S7.

treatment, we asked whether the observed changes derived from the dry skin treatment per se or from dry-skin-evoked scratching (Wilson et al., 2013). To address this question, we used a dry-skin-induced chronic itch model in a caudal back assay (Figures S7B and S7C), which effectively prevents AEW-treated mice from scratching the administration site (Wilson et al., 2013). Interestingly, in the caudal back model of dry skin, both WT and ASIC3 KO mice developed similar off-site scratching behavior in response to AEW treatment (Figure S7D). In addition, the ASIC3 KO and WT mice also displayed comparable epidermal hyperplasia (Figures S7E and S7F) at the AEW-treated site, suggesting that scratching is a major contributor of ASIC3-mediated epidermal hyperplasia in response to chronic itch. Taken together, we have established a pivotal role of ASIC3 channels in both itch behavior and scratching-dependent skin abnormalities (Figure 7G) underlying the development of dry-skin-induced chronic itch, in addition to the transduction of acute itch evoked via coincident stimulation by acidosis and compounds that target the nonproton ligand-sensing domain of the channel.

DISCUSSION

Chronic itch that is insensitive to antihistamine treatment is a major manifestation of multiple skin and systemic diseases. In this study, we demonstrate that acidosis potentiates the itch response (Figures 1 and 2) evoked by SL-NH_2, but not BAM8-22, in a manner dependent on ASIC3, but not ASIC1a, channels (Figure 3). Prolonged activation of ASIC3 channels via coincident detection of acidosis and SL-NH_2 (Figure 4) appears to be responsible for the acid potentiation of itch. This is supported by the finding that similar to SL-NH_2, co-application of acid with NPFF, an endogenous peptide that enhances proton-evoked sustained ASIC3 currents (Askwith et al., 2000), and injection of GMQ, which causes sustained activation of ASIC3 channels at neutral pH, both increased scratching behaviors in an ASIC3-dependent manner (Figure 5). Finally, ASIC3-deficient animals displayed substantially less scratching behavior and pathological changes in the dry skin pruritus model (Figures 6 and 7). Together, we have established a critical role of ASIC3 in acute and chronic itch sensation and revealed a mechanism of itch transduction via sustained ASIC3 channel activation resulting from coincident stimulation by acidosis and compounds that act at the nonproton ligand-sensing domain of the channel. Our data suggest that this form of noxious sensation includes both itch and pain. In this regard, ASIC3 may be an ideal therapeutic target of itch and pain associated with skin and systematic diseases.

Neuropeptides, together with their targeted receptor signaling pathways, are emerging as a group of key regulators of acute and chronic itch (Bautista et al., 2014; Han and Dong, 2014; Ikoma et al., 2006). Commonly known endogenous peptide pruritogens, such as endothelin-1, thymic stromal lymphopoietic protein (TSLP), and BAM8-22, signal via distinct molecular pathways to evoke robust scratching behaviors (Bautista et al., 2014; Han and Dong, 2014; Ikoma et al., 2006). SL-NH_2 is a natural peptide derived from a tethered ligand sequence of PAR2. It is possible that soluble SL-NH_2 peptide is produced from PAR2 by cleavage of the SLIGRL sequence (Liu et al., 2011), which in turn activates both PAR2 and MrgprC11. Although PAR2 does not directly mediate itch, it can modulate inflammatory responses (Ramachandran and Hollenberg, 2008), which typically include tissue acidosis. Thus, in addition to eliciting itch responses through the classical itch receptor MrgprC11 (Liu et al., 2011), SL-NH_2 can also induce itch through ASIC3 channels under inflammatory conditions with tissue acidosis. Similar to SL-NH_2, neuropeptides with common C-terminal motifs, such

as -RFamide, -RYamide, or -RYG, which can be released from mast cells (Lee et al., 2008), also activate MrgprC11 (Han et al., 2002) and thought to facilitate allergic itch. A number of these immune cell-derived peptides also potentiated acid-induced ASIC3 sustained currents (Askwith et al., 2000). As we showed for NPFF in the current study, these endogenous peptides may also contribute to allergic itch by prolonging ASIC3 activation under acidosis (Figure 7G).

In the dry skin chronic itch model, we demonstrated the ASIC3-dependent itch response and epidermal hyperplasia in two scratchable surface areas (i.e., rostral back/neck and cheek; Figures 6 and 7), but not the non-scratchable area (caudal back; Figures S7B–S7F), indicating that scratching of the affected skin area is essential for the ASIC3-depenedent phenotypes. This probably reflects the need for inflammation (and the accompanied tissue acidosis), an inevitable consequence of scratching the damaged skin, to induce ASIC3 activity. Being integral components of inflammation, the PAR2- and immune cell-derived peptides then further potentiate the acid-induced currents, leading to the ASIC3-dependent itch sensation (Figure 7G). Interestingly, the dry skin treatment led to upregulated expression of several well-established itch receptors (TRPA1, MrgprC11, and MrgprA3) in sensory neurons of WT, but not ASIC3 KO, mice (Figures 6F–6I). Together with the finding that ablating TRPV1-positive neurons, which should include all TRPA1-positive ones, abolished the ASIC3-mediated itch response (data not shown), these results suggest that the same neurons that mediate histamine-independent itch are likely also involved in the ASIC3-mediated itch sensation. In fact, TRPA1 is believed to be required for chronic itch, as either pharmacological inhibition or genetic deletion of TRPA1 channels abolishes dry-skin-evoked itch behaviors (Wilson et al., 2013).

The present findings support the notion that ASIC3 channels are indeed involved in itch in addition to nociception (Chen et al., 2002; Deval et al., 2008; Li and Xu, 2011; Sluka et al., 2003) and also question the relationship between acidosis-associated itch and pain. By employing the cheek assay and itch model (Figure 2), we verified that SL-NH_2 indeed acts as a pruritogen over an algogen, while acid acts more like an algogen rather than a pruritogen, in an ASIC3-independent and dependent manner, respectively. Strikingly, combined acidosis and SL-NH_2 enhances both scratching (itch) and wiping (pain) behaviors in an ASIC3-dependent manner. Furthermore, the concurrent manifestation of pain and itch was also observed in the cheek model of dry-skin-induced chronic itch in WT, but not ASIC3 KO, mice (Figure 7). Interestingly, MrgprC11 has been proposed to participate in not only itch (Liu et al., 2009, 2011) but also hyperalgesia (Guan et al., 2010). The relationship between itch and pain remains an active area of investigation in somatosensation. It should be further examined whether ASIC3-mediated itch/pain sensation represents a new form of sensory modality with special implications in physiology and pathology. Indeed, inflammation (Mamet et al., 2002; Voilley et al., 2001) or dry skin treatment (Figure 6F) strongly enhances ASIC3 transcription, which exacerbates the scratching behavior associated with chronic itch. Moreover, ASIC3 also physically interacts with P2X receptors to concurrently sense acid and ATP a mechanism with significance in ischemic pain (Birdsong et al., 2010). Elucidating the molecular mechanisms underlying ASIC3-mediated itch transduction is the first step toward understanding the complex relationship between pain and itch. The pathological implications of ASIC3 channels indicate that pharmacological inhibition of these channels may represent a strategy to treat itch under certain pathological conditions.

EXPERIMENTAL PROCEDURES

Animals and Itch-Related Behavioral Assays

Animal care and the experimental protocol were approved by the Animal Ethics Committee of Shanghai Jiao Tong University School of Medicine, Shanghai, China. All behavioral measurements were performed in awake and unrestrained C57BL/6J (obtained from Shanghai Slac Laboratory Animal Company), WT, and ASIC3 KO littermates (Price et al., 2001), or WT and ASIC1a KO littermates (Wemmie et al., 2002) (male, 2–3 months old, C57BL/6 background). While acute itch behaviors in the neck model indexed by the number of scratching bouts were evaluated as described previously (Liu et al., 2009), those in the cheek model were performed following a procedure similar to that previously described (Shimada and LaMotte, 2008). The mouse model of chronic itch was adapted from a previously reported model of experimental dry skin (Miyamoto et al., 2002; Wilson et al., 2013). All behavioral experiments were conducted and scored with the experimenter blinded to the genotype and the drug treatment.

Cell Culture and Transfection

All constructs were expressed in CHO cells as reported previously (Yu et al., 2010). DRG neurons (C1-T1) were prepared as previously described (Wang et al., 2013).

Electrophysiology

Electrophysiological recordings were performed using conventional whole-cell and macropatch configurations under voltage clamp as described previously (Wang et al., 2013).

Histology

Skin specimens were dissected immediately after animals were killed and fixed in 4% paraformaldehyde overnight at 4°C, dehydrated in 70% ethanol, and embedded in optimal cutting temperature (OCT) compound (Tissue-Tek). Sections (10 μm) were stained with H&E. Slides were imaged with a bright-field microscope outfitted with 10×, 0.3 numerical aperture (NA), and 20×, 0.45 NA lenses (IX71, Olympus). All specimens were blinded with respect to genotype and treatment before imaging. The thickness of nucleated epidermal layers was measured using Image J software from 20× bright-field images taken at two or three randomly selected fields per section.

Reagents

All drugs were purchased from Sigma-Aldrich unless otherwise mentioned. SL-NH_2 and analogous peptides were synthesized by GL Biochem.

Real-Time RT-PCR

DRGs (C1-T1) were dissected and total RNA was extracted using TRIzol reagent (Life Technologies). 6 μg total RNA was used as a template for cDNA synthesis and amplification with the SuperScript III First-Stand Synthesis System (Life Technologies) according to the manufacturer's instructions.

Site-Directed Mutagenesis

Site-directed mutagenesis of plasmid was performed as described previously (Yu et al., 2010). Mutations were made using the Quik-Change mutagenesis kit (Stratagene) according to the manufacturer's protocol.

Data Analysis

Results are expressed as the mean ± SEM. Statistical comparisons were performed using unpaired or paired Student's t tests or two-way repeated-measures ANOVA. $p < 0.05$, $p < 0.01$, and $p < 0.001$ represent statistically significant differences. Current decay kinetics (Cushman et al., 2007) were fit with

a single exponential: $I = I_0 + Ae^{-t/\tau}$, where τ is the time constant of desensitization. The sustained ASIC3 currents (Wang et al., 2013) were measured at 10 s after the start of acid application.

SUPPLEMENTAL INFORMATION

Supplemental Information includes Supplemental Results, Supplemental Experimental Procedures, and seven figures and can be found with this article online at http://dx.doi.org/10.1016/j.celrep.2015.09.002.

AUTHOR CONTRIBUTIONS

T.-L.X., W.-G.L., and Z.P. designed the project. Z.P., W.-G.L., C.H., Y.-M.J., and X.W. performed cell culture, patch-clamp recordings, and behavior testing. Z.P. and W.-G.L. did data analysis. W.-G.L., X.C., M.X.Z., and T.-L.X wrote the manuscript. All authors read and approved the final manuscript.

ACKNOWLEDGMENTS

We thank Ms. Yan-Qin Hu and Ying Li for their technique assistance. We thank Drs. Ming-Gang Liu, Bo Duan, Jianguo Gu, and James Celentano for discussion. This study was supported by grants from the National Basic Research Program of China (2014CB910300), the National Natural Science Foundation of China (31230028, 81400870, 81500941, 91132303, and 313111222).

Received: March 21, 2015
Revised: July 20, 2015
Accepted: August 31, 2015
Published: October 1, 2015

REFERENCES

Akiyama, T., Carstens, M.I., and Carstens, E. (2010). Differential itch- and pain-related behavioral responses and μ-opoid modulation in mice. Acta Derm. Venereol. *90*, 575–581.

Alvarez de la Rosa, D., Zhang, P., Shao, D., White, F., and Canessa, C.M. (2002). Functional implications of the localization and activity of acid-sensitive channels in rat peripheral nervous system. Proc. Natl. Acad. Sci. USA *99*, 2326–2331.

Askwith, C.C., Cheng, C., Ikuma, M., Benson, C., Price, M.P., and Welsh, M.J. (2000). Neuropeptide FF and FMRFamide potentiate acid-evoked currents from sensory neurons and proton-gated DEG/ENaC channels. Neuron *26*, 133–141.

Baconguis, I., Bohlen, C.J., Goehring, A., Julius, D., and Gouaux, E. (2014). X-ray structure of acid-sensing ion channel 1-snake toxin complex reveals open state of a Na(+)-selective channel. Cell *156*, 717–729.

Bautista, D.M., Wilson, S.R., and Hoon, M.A. (2014). Why we scratch an itch: the molecules, cells and circuits of itch. Nat. Neurosci. *17*, 175–182.

Birdsong, W.T., Fierro, L., Williams, F.G., Spelta, V., Naves, L.A., Knowles, M., Marsh-Haffner, J., Adelman, J.P., Almers, W., Elde, R.P., and McCleskey, E.W. (2010). Sensing muscle ischemia: coincident detection of acid and ATP via interplay of two ion channels. Neuron *68*, 739–749.

Bohlen, C.J., Chesler, A.T., Sharif-Naeini, R., Medzihradszky, K.F., Zhou, S., King, D., Sánchez, E.E., Burlingame, A.L., Basbaum, A.I., and Julius, D. (2011). A heteromeric Texas coral snake toxin targets acid-sensing ion channels to produce pain. Nature *479*, 410–414.

Chen, C.C., Zimmer, A., Sun, W.H., Hall, J., Brownstein, M.J., and Zimmer, A. (2002). A role for ASIC3 in the modulation of high-intensity pain stimuli. Proc. Natl. Acad. Sci. USA *99*, 8992–8997.

Chiang, P.H., Chien, T.C., Chen, C.C., Yanagawa, Y., and Lien, C.C. (2015). ASIC-dependent LTP at multiple glutamatergic synapses in amygdala network is required for fear memory. Sci. Rep. *5*, 10143.

Cushman, K.A., Marsh-Haffner, J., Adelman, J.P., and McCleskey, E.W. (2007). A conformation change in the extracellular domain that accompanies desensitization of acid-sensing ion channel (ASIC) 3. J. Gen. Physiol. *129*, 345–350.

Deval, E., Noël, J., Lay, N., Alloui, A., Diochot, S., Friend, V., Jodar, M., Lazdunski, M., and Lingueglia, E. (2008). ASIC3, a sensor of acidic and primary inflammatory pain. EMBO J. *27*, 3047–3055.

Du, J., Reznikov, L.R., Price, M.P., Zha, X.M., Lu, Y., Moninger, T.O., Wemmie, J.A., and Welsh, M.J. (2014). Protons are a neurotransmitter that regulates synaptic plasticity in the lateral amygdala. Proc. Natl. Acad. Sci. USA *111*, 8961–8966.

Frey Law, L.A., Sluka, K.A., McMullen, T., Lee, J., Arendt-Nielsen, L., and Graven-Nielsen, T. (2008). Acidic buffer induced muscle pain evokes referred pain and mechanical hyperalgesia in humans. Pain *140*, 254–264.

Friese, M.A., Craner, M.J., Etzensperger, R., Vergo, S., Wemmie, J.A., Welsh, M.J., Vincent, A., and Fugger, L. (2007). Acid-sensing ion channel-1 contributes to axonal degeneration in autoimmune inflammation of the central nervous system. Nat. Med. *13*, 1483–1489.

Fromy, B., Lingueglia, E., Sigaudo-Roussel, D., Saumet, J.L., and Lazdunski, M. (2012). Asic3 is a neuronal mechanosensor for pressure-induced vasodilation that protects against pressure ulcers. Nat. Med. *18*, 1205–1207.

Gao, J., Duan, B., Wang, D.G., Deng, X.H., Zhang, G.Y., Xu, L., and Xu, T.L. (2005). Coupling between NMDA receptor and acid-sensing ion channel contributes to ischemic neuronal death. Neuron *48*, 635–646.

Gavva, N.R., Tamir, R., Klionsky, L., Norman, M.H., Louis, J.C., Wild, K.D., and Treanor, J.J. (2005). Proton activation does not alter antagonist interaction with the capsaicin-binding pocket of TRPV1. Mol. Pharmacol. *68*, 1524–1533.

Guan, Y., Liu, Q., Tang, Z., Raja, S.N., Anderson, D.J., and Dong, X. (2010). Mas-related G-protein-coupled receptors inhibit pathological pain in mice. Proc. Natl. Acad. Sci. USA *107*, 15933–15938.

Han, L., and Dong, X. (2014). Itch mechanisms and circuits. Annu. Rev. Biophys. *43*, 331–355.

Han, S.K., Dong, X., Hwang, J.I., Zylka, M.J., Anderson, D.J., and Simon, M.I. (2002). Orphan G protein-coupled receptors MrgA1 and MrgC11 are distinctively activated by RF-amide-related peptides through the Galpha q/11 pathway. Proc. Natl. Acad. Sci. USA *99*, 14740–14745.

Ikoma, A., Steinhoff, M., Ständer, S., Yosipovitch, G., and Schmelz, M. (2006). The neurobiology of itch. Nat. Rev. Neurosci. *7*, 535–547.

Imamachi, N., Park, G.H., Lee, H., Anderson, D.J., Simon, M.I., Basbaum, A.I., and Han, S.K. (2009). TRPV1-expressing primary afferents generate behavioral responses to pruritogens via multiple mechanisms. Proc. Natl. Acad. Sci. USA *106*, 11330–11335.

Kellenberger, S., and Schild, L. (2015). International Union of Basic and Clinical Pharmacology. XCI. structure, function, and pharmacology of acid-sensing ion channels and the epithelial Na+ channel. Pharmacol. Rev. *67*, 1–35.

Kreple, C.J., Lu, Y., Taugher, R.J., Schwager-Gutman, A.L., Du, J., Stump, M., Wang, Y., Ghobbeh, A., Fan, R., Cosme, C.V., et al. (2014). Acid-sensing ion channels contribute to synaptic transmission and inhibit cocaine-evoked plasticity. Nat. Neurosci. *17*, 1083–1091.

Krishtal, O. (2003). The ASICs: signaling molecules? Modulators? Trends Neurosci. *26*, 477–483.

LaMotte, R.H., Dong, X., and Ringkamp, M. (2014). Sensory neurons and circuits mediating itch. Nat. Rev. Neurosci. *15*, 19–31.

Lee, M.G., Dong, X., Liu, Q., Patel, K.N., Choi, O.H., Vonakis, B., and Undem, B.J. (2008). Agonists of the MAS-related gene (Mrgs) orphan receptors as novel mediators of mast cell-sensory nerve interactions. J. Immunol. *180*, 2251–2255.

Lembo, P.M., Grazzini, E., Groblewski, T., O'Donnell, D., Roy, M.O., Zhang, J., Hoffert, C., Cao, J., Schmidt, R., Pelletier, M., et al. (2002). Proenkephalin A gene products activate a new family of sensory neuron–specific GPCRs. Nat. Neurosci. *5*, 201–209.

Li, W.G., and Xu, T.L. (2011). ASIC3 channels in multimodal sensory perception. ACS Chem. Neurosci. *2*, 26–37.

Liu, Q., Tang, Z., Surdenikova, L., Kim, S., Patel, K.N., Kim, A., Ru, F., Guan, Y., Weng, H.J., Geng, Y., et al. (2009). Sensory neuron-specific GPCR Mrgprs are itch receptors mediating chloroquine-induced pruritus. Cell *139*, 1353–1365.

Liu, Q., Weng, H.J., Patel, K.N., Tang, Z., Bai, H., Steinhoff, M., and Dong, X. (2011). The distinct roles of two GPCRs, MrgprC11 and PAR2, in itch and hyperalgesia. Sci. Signal. *4*, ra45.

Liu, Q., Sikand, P., Ma, C., Tang, Z., Han, L., Li, Z., Sun, S., LaMotte, R.H., and Dong, X. (2012). Mechanisms of itch evoked by β-alanine. J. Neurosci. *32*, 14532–14537.

Mamet, J., Baron, A., Lazdunski, M., and Voilley, N. (2002). Proinflammatory mediators, stimulators of sensory neuron excitability via the expression of acid-sensing ion channels. J. Neurosci. *22*, 10662–10670.

Miyamoto, T., Nojima, H., Shinkado, T., Nakahashi, T., and Kuraishi, Y. (2002). Itch-associated response induced by experimental dry skin in mice. Jpn. J. Pharmacol. *88*, 285–292.

Nystedt, S., Larsson, A.K., Aberg, H., and Sundelin, J. (1995). The mouse proteinase-activated receptor-2 cDNA and gene. Molecular cloning and functional expression. J. Biol. Chem. *270*, 5950–5955.

Price, M.P., McIlwrath, S.L., Xie, J., Cheng, C., Qiao, J., Tarr, D.E., Sluka, K.A., Brennan, T.J., Lewin, G.R., and Welsh, M.J. (2001). The DRASIC cation channel contributes to the detection of cutaneous touch and acid stimuli in mice. Neuron *32*, 1071–1083.

Qu, L., Fan, N., Ma, C., Wang, T., Han, L., Fu, K., Wang, Y., Shimada, S.G., Dong, X., and LaMotte, R.H. (2014). Enhanced excitability of MRGPRA3- and MRGPRD-positive nociceptors in a model of inflammatory itch and pain. Brain *137*, 1039–1050.

Ramachandran, R., and Hollenberg, M.D. (2008). Proteinases and signalling: pathophysiological and therapeutic implications via PARs and more. Br. J. Pharmacol. *153* (*Suppl 1*), S263–S282.

Reeh, P.W., and Steen, K.H. (1996). Tissue acidosis in nociception and pain. Prog. Brain Res. *113*, 143–151.

Shim, W.S., Tak, M.H., Lee, M.H., Kim, M., Kim, M., Koo, J.Y., Lee, C.H., Kim, M., and Oh, U. (2007). TRPV1 mediates histamine-induced itching via the activation of phospholipase A2 and 12-lipoxygenase. J. Neurosci. *27*, 2331–2337.

Shimada, S.G., and LaMotte, R.H. (2008). Behavioral differentiation between itch and pain in mouse. Pain *139*, 681–687.

Sluka, K.A., Price, M.P., Breese, N.M., Stucky, C.L., Wemmie, J.A., and Welsh, M.J. (2003). Chronic hyperalgesia induced by repeated acid injections in muscle is abolished by the loss of ASIC3, but not ASIC1. Pain *106*, 229–239.

Steen, K.H., and Reeh, P.W. (1993). Sustained graded pain and hyperalgesia from harmless experimental tissue acidosis in human skin. Neurosci. Lett. *154*, 113–116.

Sutherland, S.P., Benson, C.J., Adelman, J.P., and McCleskey, E.W. (2001). Acid-sensing ion channel 3 matches the acid-gated current in cardiac ischemia-sensing neurons. Proc. Natl. Acad. Sci. USA *98*, 711–716.

Vergo, S., Craner, M.J., Etzensperger, R., Attfield, K., Friese, M.A., Newcombe, J., Esiri, M., and Fugger, L. (2011). Acid-sensing ion channel 1 is involved in both axonal injury and demyelination in multiple sclerosis and its animal model. Brain *134*, 571–584.

Voilley, N., de Weille, J., Mamet, J., and Lazdunski, M. (2001). Nonsteroid anti-inflammatory drugs inhibit both the activity and the inflammation-induced expression of acid-sensing ion channels in nociceptors. J. Neurosci. *21*, 8026–8033.

Waldmann, R., Bassilana, F., de Weille, J., Champigny, G., Heurteaux, C., and Lazdunski, M. (1997a). Molecular cloning of a non-inactivating proton-gated Na+ channel specific for sensory neurons. J. Biol. Chem. *272*, 20975–20978.

Waldmann, R., Champigny, G., Bassilana, F., Heurteaux, C., and Lazdunski, M. (1997b). A proton-gated cation channel involved in acid-sensing. Nature *386*, 173–177.

Wang, X., Li, W.G., Yu, Y., Xiao, X., Cheng, J., Zeng, W.Z., Peng, Z., Xi Zhu, M., and Xu, T.L. (2013). Serotonin facilitates peripheral pain sensitivity in a manner that depends on the nonproton ligand sensing domain of ASIC3 channel. J. Neurosci. *33*, 4265–4279.

Wemmie, J.A., Chen, J., Askwith, C.C., Hruska-Hageman, A.M., Price, M.P., Nolan, B.C., Yoder, P.G., Lamani, E., Hoshi, T., Freeman, J.H., Jr., and Welsh, M.J. (2002). The acid-activated ion channel ASIC contributes to synaptic plasticity, learning, and memory. Neuron *34*, 463–477.

Wilson, S.R., Gerhold, K.A., Bifolck-Fisher, A., Liu, Q., Patel, K.N., Dong, X., and Bautista, D.M. (2011). TRPA1 is required for histamine-independent, Mas-related G protein-coupled receptor-mediated itch. Nat. Neurosci. *14*, 595–602.

Wilson, S.R., Nelson, A.M., Batia, L., Morita, T., Estandian, D., Owens, D.M., Lumpkin, E.A., and Bautista, D.M. (2013). The ion channel TRPA1 is required for chronic itch. J. Neurosci. *33*, 9283–9294.

Xiong, Z.G., Zhu, X.M., Chu, X.P., Minami, M., Hey, J., Wei, W.L., MacDonald, J.F., Wemmie, J.A., Price, M.P., Welsh, M.J., and Simon, R.P. (2004). Neuroprotection in ischemia: blocking calcium-permeable acid-sensing ion channels. Cell *118*, 687–698.

Yu, Y., Chen, Z., Li, W.G., Cao, H., Feng, E.G., Yu, F., Liu, H., Jiang, H., and Xu, T.L. (2010). A nonproton ligand sensor in the acid-sensing ion channel. Neuron *68*, 61–72.

Yu, Y., Li, W.G., Chen, Z., Cao, H., Yang, H., Jiang, H., and Xu, T.L. (2011). Atomic level characterization of the nonproton ligand-sensing domain of ASIC3 channels. J. Biol. Chem. *286*, 24996–25006.

Ziemann, A.E., Schnizler, M.K., Albert, G.W., Severson, M.A., Howard, M.A., 3rd, Welsh, M.J., and Wemmie, J.A. (2008). Seizure termination by acidosis depends on ASIC1a. Nat. Neurosci. *11*, 816–822.